Journal of Inflammation Research

Dovepress
Taylor & Francis Group

Open Access Full Text Article

ORIGINAL RESEARCH

Angiotensin-(1-7) Inhibits Angiogenesis and Alleviates Joint Damage in CIA Mice via the Hippo–YAP Pathway

Shan Zhang, Min Sheng, Dan Yu, Kechen Qian, Yichen Zhang, Wenhan Huang, Feifeng Ren, Lin Tang

Department of Rheumatology and Immunology, Second Affiliated Hospital of Chongqing Medical University, Chongqing, People's Republic of China

Correspondence: Lin Tang, Department of Rheumatology and Immunology, Second Affiliated Hospital of Chongqing Medical University, No. 76 Linjiang Road, Yuzhong District, Chongqing, 400010, People's Republic of China, Email hopetang@hospital.cqmu.edu.cn

Purpose: Angiotensin-(1-7) [Ang-(1-7)], a bioactive peptide of the renin–angiotensin system, exerts potent anti-inflammatory, antifibrotic and metabolic regulatory effects. Ang-(1-7) inhibits synovial inflammation and bone destruction in collagen-induced arthritis (CIA) model mice, but its role in rheumatoid arthritis (RA) angiogenesis remains unknown. This study aimed to investigate the effect of Ang-(1-7) on synovial angiogenesis in CIA mice.

Methods: Arthritis scores and histopathology were used to assess the anti-inflammatory and joint damage-alleviating effects of Ang-(1-7) in CIA mice. Immunohistochemistry and immunofluorescence were used to detect vascular density in the synovium of CIA mice. The proliferation, migration, and tube formation abilities and the expression of angiogenic mediators of tumor necrosis factor-alpha (TNF-α)-induced human umbilical vein endothelial cells (HUVECs) were examined to assess Ang-(1-7) antiangiogenic activity. Immunofluorescence and Western blotting were used to analyze the protein levels, phosphorylation, and nuclear translocation of large tumor suppressor kinase 1 (LATS1) and Yes-associated protein (YAP) in CIA mice and TNF-α-induced HUVECs.

Results: Ang-(1-7) treatment significantly reduced systemic inflammation in CIA mice, inhibited angiogenesis in the synovium, and attenuated synovial hyperplasia, inflammatory cell infiltration, and cartilage destruction. Ang-(1-7) also inhibited TNF-α-induced HUVEC proliferation, migration, and tube formation. Mechanistic investigations revealed that Ang-(1-7) exerted its therapeutic effects through modulation of the Hippo–YAP pathway. Ang-(1-7) significantly downregulated LATS1 and YAP expression while restoring their phosphorylation status. Furthermore, Ang-(1-7) inhibited YAP nuclear translocation, subsequently suppressing downstream targets, including hypoxia-inducible factor-1 (HIF-1), vascular endothelial growth factor (VEGF), and VEGF receptor 2 (VEGFR2). The effects of Ang-(1-7) were partially blocked by the Mas receptor antagonist A779.

Conclusion: Ang-(1-7) acts on the Mas receptor to regulate Hippo–YAP signaling, inhibit YAP activation, and suppress the production of HIF-1, VEGF and VEGFR2. This leads to the suppression of TNF-α-stimulated HUVEC activity, thereby attenuating synovial angiogenesis, inflammation, and joint damage in CIA mice.

Keywords: Angiotensin-(1-7), Mas receptor, arthritis, angiogenesis, hippo–YAP signaling pathway

Introduction

Rheumatoid arthritis (RA) is a systemic autoimmune disease that primarily affects joints and has a global prevalence of 0.25%–1%. It can lead to disability and deformity and often requires lifelong treatment.[1,2] The main pathological features of RA include immune activation, synovial inflammation, and proliferation, along with angiogenesis, resulting in aggressive pannus formation that eventually causes cartilage and bone destruction.[3] Angiogenesis is a key marker of RA progression and is often considered a sign of the transition from acute to chronic inflammation.[4] New blood vessels provide oxygen and nutrients to proliferating inflammatory cells, maintaining the chronic inflammatory state in RA.[5] Moreover, neovascularization activates synovial fibroblasts (FLSs) and promotes osteoclast formation, leading to joint deformity and functional impairment.[6] As a pivotal pathological bridge between inflammatory activation and osteoclastic bone erosion, excessive synovial angiogenesis represents a promising therapeutic avenue in RA management.

Received: 21 May 2025
Accepted: 3 August 2025
Published: 10 September 2025

Ang-(1-7) is an important effector molecule in the renin–angiotensin system. It is produced mainly via the hydrolysis of angiotensin II (Ang II) by angiotensin converting enzyme 2 (ACE2) and functions through activation of the Mas receptor.[7] Our previous research confirmed that the ACE2/Ang-(1-7)/Mas axis has anti-inflammatory, metabolism-regulating, and antifibrotic effects in models of sepsis and pulmonary fibrosis.[8,9] We also demonstrated that the ACE2/Ang-(1-7)/Mas axis inhibits the activation of the MAPK and NF-κB signaling pathways in the ankle joints of collagen-induced arthritis (CIA) model mice, attenuating inflammation and bone destruction.[10] Additionally, some studies have shown that in certain cancers, such as nasopharyngeal carcinoma, lung adenocarcinoma, and hepatocellular carcinoma, Ang-(1-7) exerts antitumor effects by inhibiting angiogenesis; reducing the expression of angiogenic factors; suppressing tumor cell proliferation, migration, and invasion; and inducing autophagy in tumor cells.[11–16] However, no studies have confirmed whether Ang-(1-7) regulates synovial angiogenesis in RA.

The Hippo-YAP signaling pathway serves as a critical regulator of angiogenesis, modulating endothelial cell proliferation, migration, and survival to orchestrate vascular sprouting, barrier formation, and network remodeling.[17,18] Importantly, this pathway also plays a pivotal role in RA, where its dysregulation contributes to synovial pathology and FLS activation. Studies have shown that Yes-associated protein (YAP) and transcriptional coactivator with PDZ-binding motif (TAZ) are upregulated in RA-FLSs and that the knockdown of YAP and TAZ can inhibit RA-FLS migration and invasion by inducing autophagy.[19] The YAP inhibitor verteporfin has been shown to significantly suppress the invasive phenotype of FLSs, attenuate synovial hyperplasia in adjuvant-induced arthritis rats, and decrease the severity of arthritis.[20] Recent studies have shown that Ang II binds AT1R to activate YAP in human umbilical vein endothelial cells (HUVECs), promoting endothelial–mesenchymal transition and exacerbating liver fibrosis.[21] Since the Ang-(1-7)/Mas axis usually antagonizes the Ang II/AT1R axis, We hypothesized that Ang-(1-7) attenuates pathological angiogenesis through Hippo-YAP pathway-mediated regulation of vascular endothelial cell activation.

Our study confirmed that Ang-(1-7) acts on the Mas receptor to restore Hippo pathway phosphorylation, inhibiting YAP activation and nuclear translocation in vascular endothelial cells. This suppresses vascular endothelial cell proliferation, migration, and tube formation, which inhibits angiogenesis in the RA synovium and thereby alleviates RA-associated joint damage. In conclusion, the results of this study indicate that Ang-(1-7) may represent a new target for RA intervention and provide a theoretical basis for alleviating RA by inhibiting angiogenesis.

Materials and Methods

Experimental Animals and Model Establishment

All animal experiments were approved by the Institutional Animal Care and Use Committee of Chongqing Medical University and complied with national and institutional guidelines for animal welfare. Male DBA/1 mice (8–10 weeks old) were purchased from the Experimental Animal Center of Chongqing Medical University and housed in a specific-pathogen-free (SPF) facility (temperature 20–24°C, humidity 40–60%) with a 12-hour light/dark cycle and free access to food and water.

The CIA model was established in DBA/1 mice via immunization on Days 1 and 21.[10] Briefly, chicken type II collagen was mixed with an equal volume of complete Freund's adjuvant to form an emulsion, and 0.1 mL was injected intradermally at the base of the tail. On Day 21, a second immunization was performed with chicken type II collagen emulsified in an equal volume of incomplete Freund's adjuvant. The control group received a subcutaneous injection of saline via the tail vein as a control. On Day 28, after unsuccessful models were excluded, the mice were randomly divided into the CIA group and the CIA+Ang-(1-7) group. From Day 28 onward, the CIA+Ang-(1-7) group received an intraperitoneal injection of Ang-(1-7) (2.0 mg/kg) once daily for 2 weeks, whereas the control and CIA groups received an intraperitoneal injection of saline as controls. On Day 42, the mice were euthanized, and blood and joints were collected for further studies. Chicken type II collagen, complete Freund's adjuvant and incomplete Freund's adjuvant were procured from Chondrex (Redmond, WA, USA), and Ang-(1–7) was procured from APExBIO (Houston, TX, USA).

Symptom Scoring

The scoring criteria for the arthritis index were as follows: two independent observers scored the arthritis index of the mice every three days. The severity of arthritis in the hind limbs was scored in a blinded manner using a five-point scoring system.

The evaluation focused on the degree of swelling in the paws and the incidence and severity of lesions in the hind limbs and tail. The details are as follows: 0 points, no swelling; 1 point, mild swelling in the toe joints; 2 points, swelling in the toe joints and ankle joints; 3 points, swelling below the ankle joint; and 4 points, swelling in all joints, including the ankle joint.[22]

Hematoxylin-Eosin (H&E) Staining and Pathological Examination

For histological analysis, the knee joints of the mice were collected, fixed in 10% buffered formalin, and decalcified with 15% ethylenediaminetetraacetic acid (EDTA). The entire knee joint was processed for paraffin embedding following standard protocols, and 5 μm thick serial sagittal sections were prepared and subjected to H&E staining. Histological analysis was performed in a blinded manner by two trained pathologists. The scoring system included four pathological features: synovial hyperplasia, inflammatory cell infiltration, pannus formation, and bone destruction. Each parameter was scored on a scale of 0 (normal) to 3 (severe).[10]

Enzyme-Linked Immunosorbent Assay (ELISA)

Commercial ELISA kits (Meimian, Jiangsu, China) were used to measure the serum levels of TNF-α (MM-0132M1), IL-6 (MM-0163M1), VEGF (MM-0128M2), and HIF-1 (MM-45345M2) according to the manufacturer's instructions.

Cell Culture

HUVECs were purchased from the Cell Bank of the Chinese Academy of Sciences (Shanghai, China) and cultured in RPMI 1640 medium (Gibco, Waltham, MA, USA) supplemented with 10% fetal bovine serum and 1% penicillin–streptomycin. The cells were cultured at 37°C in a humidified environment with 5% CO_2 and 95% O_2. HUVECs were stimulated with varying concentrations of TNF-α (2.5 ng/mL, 5 ng/mL, 10 ng/mL, 20 ng/mL, or 40 ng/mL). On the basis of previously published data[22] and preliminary results (Supplementary Figure 1), we selected 10 ng/mL TNF-α for subsequent experiments. The cells were also treated with Ang-(1-7) (0.1 μmol/L, 1 μmol/L, or 10 μmol/L) to determine the optimal concentration (Supplementary Figure 2). Prior to Ang-(1-7) (10 μmol/L) treatment for 24 hours, the cells were pretreated with A779 (10 μmol/L) or XMU-MP-1 (1 μmol/L) for 30 minutes. Recombinant mouse TNF-α (300–01A, ≥98% purity by SDS–PAGE and HPLC) was purchased from PeproTech (Cranbury, NJ, USA). A779 (B6056) was obtained from APExBIO (Houston, TX, USA), and XMU-MP-1 (HY-100526) was acquired from MedChemExpress (Monmouth Junction, NJ, USA).

5-Ethynyl-2′-Deoxyuridine (EdU) Assay

To study cell proliferation, HUVECs were seeded into 96-well plates (3×10^3 cells/well) overnight. The medium was then replaced with fresh medium containing different drug concentrations, and the mixture was incubated for 24 hours. An equal volume of EdU working solution (Abbkine, KTA2030) was subsequently added for labeling and incubated for an additional 4 hours. The cells were fixed with 4% paraformaldehyde for 15 minutes, permeabilized with 0.1% Triton X-100 for 15 minutes, and washed three times with BSA buffer. The Click-iT reaction mixture was prepared, and the samples were incubated with the mixture at room temperature in the dark. After 30 minutes, the reaction mixture was removed, and the cells were washed with BSA buffer for 5 minutes. Images were captured, and the positive cells were counted under a fluorescence microscope.

Cell Counting Kit-8 (CCK-8) Assay

A CCK-8 assay was performed to assess cell proliferation. HUVECs were seeded into 96-well plates (3×10^3 cells/well) and cultured overnight. The medium was replaced with fresh medium containing different drug concentrations, and the mixture was incubated for 24 hours. After the medium was removed, the wells were washed with PBS. A volume of 100 μL fresh complete medium and 10 μL CCK-8 reagent (Dojindo Molecular Technologies, CK04) were added to each well, followed by a 2-hour incubation. The absorbance was measured at 450 nm via a microplate reader.

Wound Healing Assay

A wound healing assay was used to analyze the migration ability of HUVECs. An appropriate number of HUVECs were seeded into 6-well plates and allowed to adhere. After adherence, the medium was replaced with fresh medium containing different drug concentrations, and the cells were cultured for 24 hours. Once the monolayer of cells reached 100% confluency, a scratch was created using a sterile pipette tip. The culture dishes were washed several times with PBS to remove debris and damaged cells. The cells were then incubated in serum-free RPMI 1640 basal medium for further culture. Images were taken at 0 and 48 hours, and cell migration was quantified via ImageJ software by calculating the wound closure area.

Transwell Migration Assay

HUVECs were suspended in serum-free medium and seeded at a density of 1×10^5 cells per well in the upper chamber of a Transwell insert (Biofil, Guangzhou, Guangdong, China). The lower chamber was filled with medium containing different drugs, and the cells were incubated for 36 hours. The migrating cells were fixed in methanol, and the upper chamber was gently wiped with a cotton swab to remove nonmigrating cells. The migrated cells were stained with 0.5% crystal violet, and images of three randomly selected areas were captured under a microscope for counting.

Tube Formation Assay

Matrigel (50 μL/well; Corning, 356234) was plated in a 96-well plate and polymerized at 37°C for 1 h. HUVECs (2×10^5 cells/mL, 100 μL/well) were seeded into Matrigel-coated wells and incubated for 6 hours. Tube-like structures were photographed under a microscope, and tube formation ability was quantified via ImageJ software by calculating the number of meshes, nodes, and total branch length.

Western Blotting

Total protein from HUVECs was extracted with RIPA lysis buffer supplemented with protease inhibitors, phosphatase inhibitors, and PMSF (Boster Biological Technology, Wuhan, Hubei, China), and the protein concentration was measured by using a BCA protein assay kit (Solarbio, PC0020-50T). Samples in SDS loading buffer were boiled, and equal amounts of protein were separated via SDS–PAGE and transferred onto PVDF membranes (Millipore Sigma, Burlington, MA, USA). The membranes were blocked at room temperature for 1 hour and incubated overnight at 4°C with primary antibodies (1:1000). The following day, the membranes were incubated with species-specific secondary antibodies (Proteintech, RGAR001) for 60 minutes. Protein–antibody complexes were visualized using an enhanced chemiluminescence (ECL) detection kit (Zenbio, Chengdu, Sichuan, China). The following primary antibodies were used: anti-VEGF (Proteintech, 19003-1-AP), anti-HIF-1 (UpingBio, YP-Ab-01776), anti-YAP (Cell Signaling Technology, 14074T), anti-p-YAP (Cell Signaling Technology, 13008T), anti-LATS (Cell Signaling Technology, 3477T), anti-p-LATS (Cell Signaling Technology, 8654S), and anti-β-actin (Proteintech, 20536-1-AP).

Quantitative Real-Time Polymerase Chain Reaction (qRT–PCR)

Total RNA was isolated from HUVECs using the SteadyPure Quick RNA Extraction Kit (Accurate Biology, AG21023) and reverse transcribed using Evo M-MLV RT reaction mix (Accurate Biology, AG11705). Gene expression was quantified with the SYBR Green Premix Pro Taq HS qPCR Kit (Accurate Biology, AG11701) and the Bio-Rad CFX96 Real-Time System. β-actin is a widely used reference gene that is stably expressed in HUVECs, making it a suitable choice as an internal control gene.[23] Reaction conditions: 95°C for 30 sec (initial denaturation), followed by 40 cycles of 95°C for 5 sec (denaturation), 60°C for 30 sec (annealing), and 72°C for 1 min (extension). Data were analyzed via the $2^{-\Delta\Delta Ct}$ method. The sequences of the primers used in this study are listed in Table 1.

Immunofluorescence Staining

HUVECs were cultured overnight on coverslips and treated with different drugs for 24 hours. The culture medium was then removed, and the cells were fixed with 4% paraformaldehyde for 15 minutes, followed by permeabilization with

Table 1 Sequences of Primers Used for qRT–PCR

Species and Gene	Forward	Reverse
Human VEGF	5′-CTTGCCTTGCTGCTCTACCT-3′	5′-AGCTGCGCTGATAGACATCC-3′
Human HIF-1	5′-CTCATCAGTTGCCACTTCCACATA-3′	5′-AGCAATTCATCTGTGCTTTCATGTC-3′
Human β-actin	5′-TGGCACCCAGCACAATGAA-3′	5′-CTAAGTCATAGTCCGCCTAGAAGCA-3′

0.5% Triton X-100 solution for 10 minutes. The cells were then incubated overnight at 4°C with a primary anti-YAP antibody (1:200; Cell Signaling Technology, 14074T). The next day, the cells were washed and incubated with a secondary antibody (1:3000, Jackson ImmunoResearch, West Grove, Pennsylvania, USA) for 1 hour and then incubated with DAPI for 5 minutes. Imaging was performed using a fluorescence microscope (Olympus, Tokyo, Japan).

On day 42 after CIA modeling, the mice were euthanized. After fixation and decalcification of the knee joints, the tissues were dehydrated in a graded ethanol series and embedded in paraffin to prepare 5 μm thick sections. The sections were deparaffinized in xylene and rehydrated with a graded ethanol series, and then antigen retrieval was performed via microwave heating for 15 minutes. The sections were blocked with BSA for 30 minutes and incubated overnight with the primary antibody. The next day, the sections were incubated with a fluorescently labeled secondary antibody for 1 hour at room temperature, and the nuclei were stained with DAPI (Beyotime, Shanghai, China). Finally, images of the sections under a fluorescence microscope were obtained and analyzed.

The following primary antibodies were used: anti-MAS1L (1:100; Proteintech, 20080-1-AP), anti-CD31 (1:1000, Abcam, ab281583), anti-VEGF (1:500, Proteintech), anti-VEGFR2 (1:1000; UpingBio Technology, YP-Ab-13245), anti-YAP (1:1000, Cell Signaling Technology), and anti-LATS (1:1000, Cell Signaling Technology).

Immunohistochemical Staining

After the samples were blocked with serum for 30 minutes, primary anti-CD31 antibody (1:1000, Abcam) was added, and the mixture was incubated overnight at 4°C. The following day, the sections were incubated with a biotin-labeled secondary antibody for 30 minutes at room temperature, followed by three washes with PBS. Streptavidin-HRP working solution was then added, followed by another three washes with PBS. The sections were stained with DAB, counterstained with hematoxylin, dehydrated in a graded ethanol series, and mounted with neutral resin. The stained tissues were finally observed under a light microscope.

Statistical Analysis

Statistical analysis was performed using GraphPad Prism 10.0.0 (GraphPad Software, San Diego, CA, USA). Each experiment was repeated at least three times. The data are presented as the means ± standard deviations (SDs). The normality of all datasets was confirmed using the Shapiro–Wilk test ($p > 0.05$ for all groups). For multiple group comparisons, one-way analysis of variance (ANOVA) was performed. Following a significant ANOVA result, Šidák's multiple comparisons test was applied to assess specific preplanned comparisons. A p value < 0.05 was considered statistically significant.

Results

Expression of the Mas Receptor in CIA Mice and HUVECs

The Mas receptor is a specific receptor for Ang-(1-7). We assessed Mas receptor expression in CIA mouse synovial tissues and HUVECs via immunofluorescence analysis. Compared with that in the control group, Mas receptor expression was significantly increased in the synovial tissues of both the CIA group and the CIA+Ang-(1-7) group, whereas Ang-(1-7) treatment did not further increase Mas receptor expression in the synovium (Figure 1A and B). Similarly, TNF-α induced an increase in Mas receptor expression in HUVECs, and Ang-(1-7) did not further increase Mas receptor expression in HUVECs (Figure 1C and D).

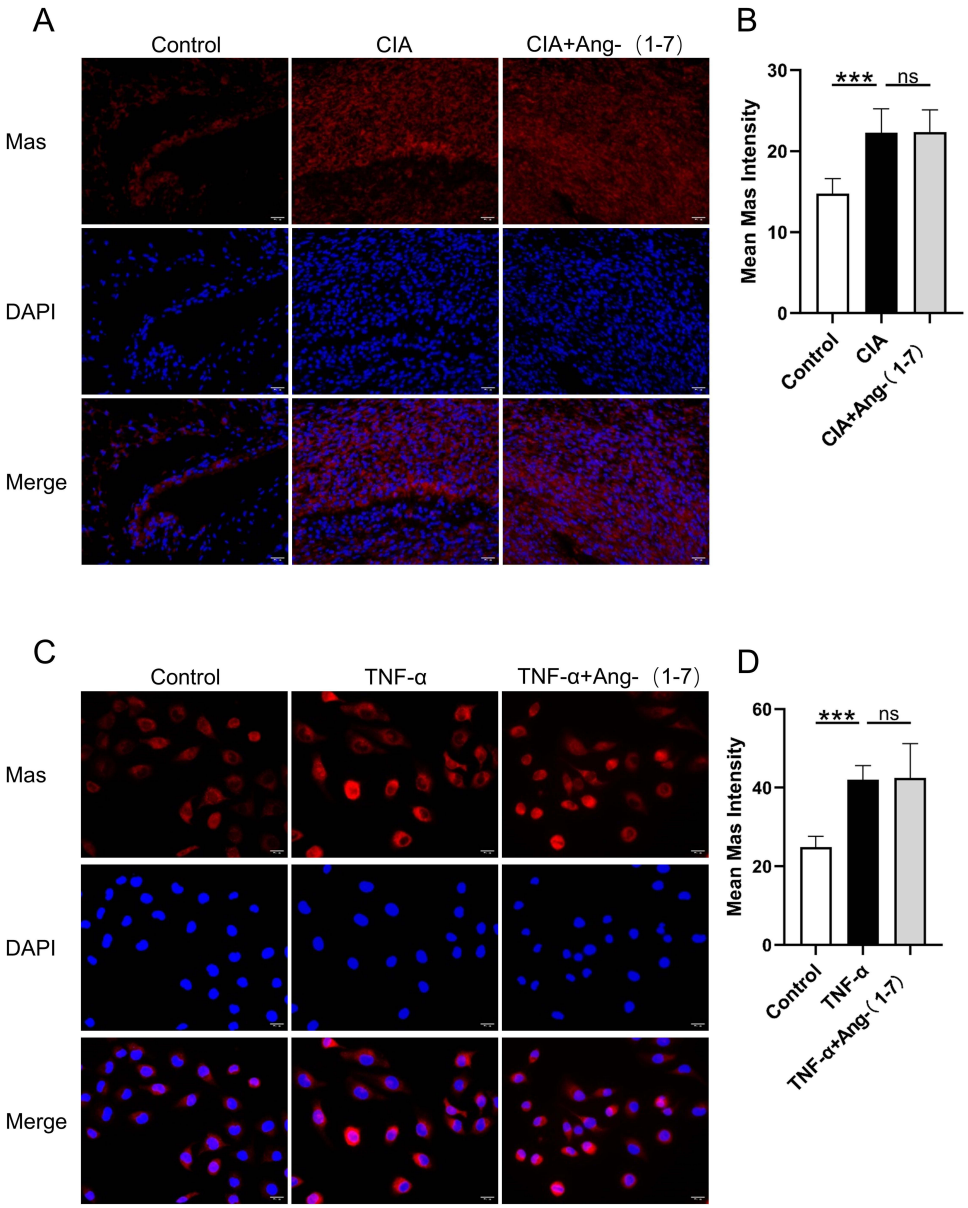

Figure 1 Immunofluorescence analysis of Mas receptor in CIA mouse synovium and TNF-α-stimulated HUVECs. (**A** and **B**) Immunofluorescence analysis of Mas receptor expression in synovial tissues (magnification: ×400, scale bar: 20 μm). The mean fluorescence intensity (MFI) of Mas was significantly higher in CIA mice compared to normal controls. Ang-(1-7) treatment (2 mg/kg/day) showed no significant modulation of Mas levels versus untreated CIA mice. (**C** and **D**) Immunofluorescence analysis of Mas receptor expression in TNF-α-induced HUVECs (magnification: ×400, scale bar: 20 μm). Mas MFI was significantly higher in TNF-α (10 ng/mL)-stimulated HUVECs compared to untreated controls. Ang-(1-7) treatment (10 μmol/L, 24 h) showed no significant modulation of Mas levels versus TNF-α-stimulated HUVECs without treatment. The results are presented as the mean ± SD (n = 5). ns: non-significant; *$p < 0.05$, **$p < 0.01$, ***$p < 0.001$.

Ang-(1-7) Alleviates Systemic Inflammation and Joint Damage in CIA Mice

Using DBA/1 mice, we established a CIA model to observe the effects of Ang-(1-7) treatment on mouse arthritis. As shown in Figure 2A, the CIA model group presented obvious redness and swelling in the joints, whereas Ang-(1-7) treatment significantly alleviated these symptoms in the CIA group (Figure 2B). H&E staining also revealed that, in CIA model mice, synovial hyperplasia invading the joint cavity was accompanied by destruction of the cartilage, extensive proliferation of synovial lining cells, increased collagen fiber proliferation, increased numbers of vascular bundles, and increased infiltration of inflammatory cells. Ang-(1-7) treatment significantly reduced the pathological scores of synovial hyperplasia, inflammatory cell infiltration, vascular formation, and bone destruction in CIA model mice (Figure 2C and D). Additionally, safranin-O and fast green staining revealed that Ang-(1-7) alleviated cartilage damage (Figure 2E). Furthermore, to assess whether Ang-(1-7) affects the secretion

of proinflammatory factors, we measured the levels of TNF-α, IL-6 and CRP in mouse serum via ELISA. The results revealed that the serum levels of TNF-α, IL-6 and CRP were significantly elevated in the CIA group. Ang-(1-7) treatment markedly reduced the serum levels of TNF-α, IL-6 and CRP in CIA mice (Figure 2F–H). Notably, Ang-(1-7) administration significantly decreased rheumatoid factor (RF) serum concentrations in CIA mice (Figure 2I). In summary, our findings indicate that Ang-(1-7) can alleviate joint damage and decrease pathological severity and inflammation levels in CIA mice.

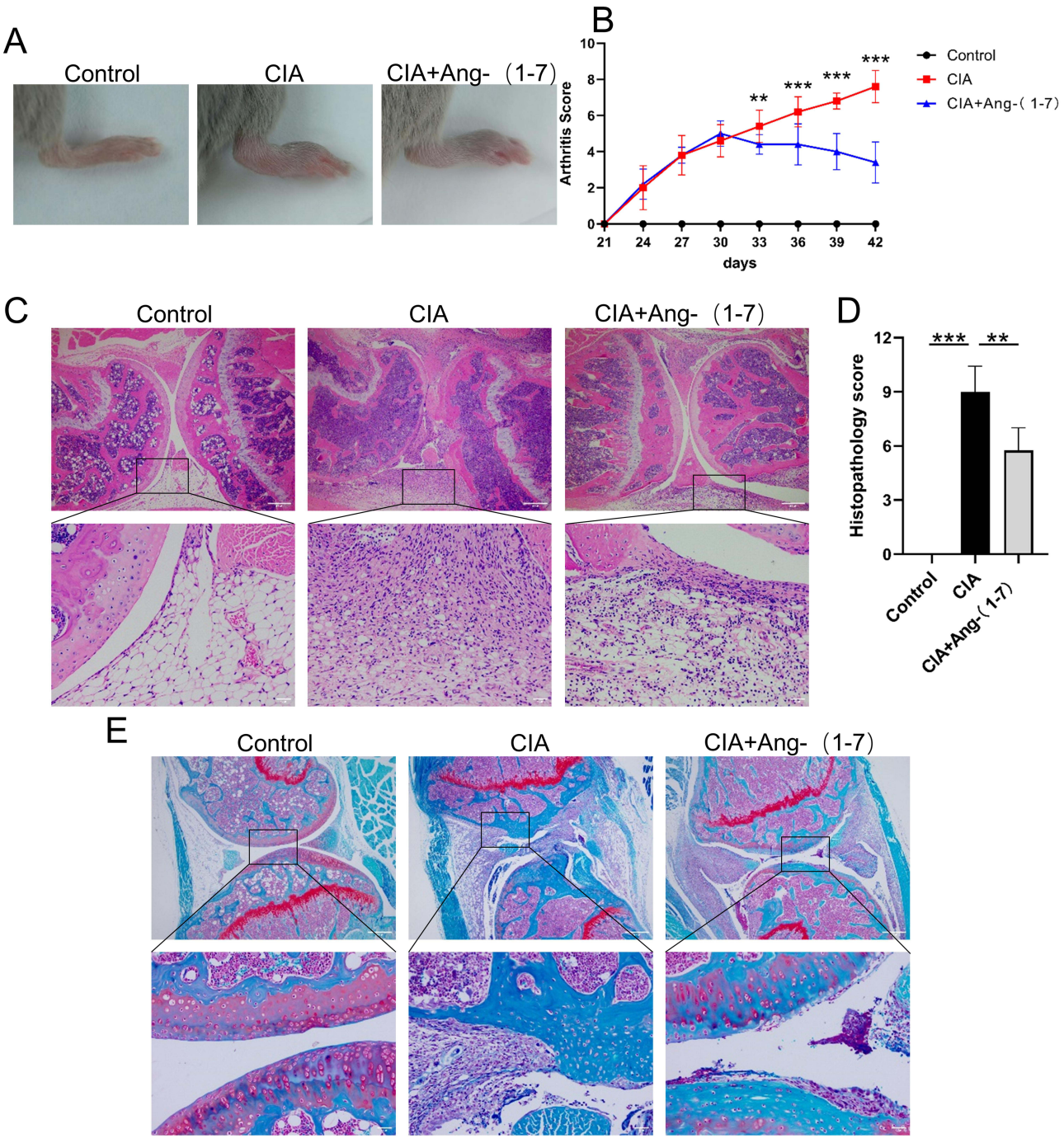

Figure 2 Continued.

https://doi.org/10.2147/JIR.S534282

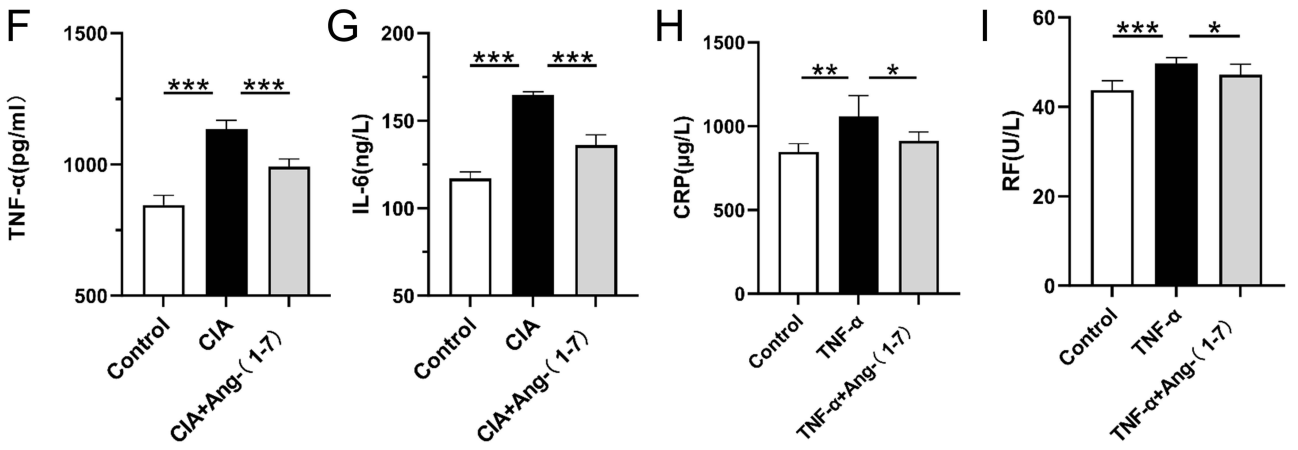

Figure 2 Ang-(1-7) effects on the in vivo model of experimental arthritis. DBA/1 mice were immunized with type II collagen emulsified in complete Freund's adjuvant (CFA; primary immunization on day 1) followed by incomplete Freund's adjuvant (IFA; booster on day 21). Mice were randomly allocated to two groups: CIA control receiving daily saline injections, or CIA+Ang-(1-7) receiving daily intraperitoneal Ang-(1-7) (2 mg/kg/day). All treatments were administered from day 28 to day 42 (14 days total). (**A**) Representative image of the paw of control mice and CIA mice, treated with and without Ang-(1-7). (**B**) Joint symptom scores were assessed every 3 days after the booster immunization until the end of the experiment. (**C**) Representative image of haematoxylin and eosin (H&E) staining (main panel: ×40, scale bar = 200 μm; inset: ×200, scale bar = 50 μm) of synovial tissues from knee joints derived from control mice, CIA mice and CIA mice treated with Ang-(1-7). (**D**) The histogram displays the mean and range of joint histopathology scores in mice. Compared to the control group, CIA mice showed a significant increase in histopathology scores, while Ang-(1-7) (2 mg/kg/day) treatment prevented this elevation. (**E**)Representative image of safranin O-fast green (SO/FG) staining (main panel: ×40, scale bar = 200 μm; inset: ×200, scale bar = 50 μm) of synovial tissues from knee joints derived from control mice, CIA mice, and CIA mice treated with Ang-(1-7).(**F-H**) ELISA analysis of serum inflammatory markers. CIA mice showed significantly increased levels of (**F**) TNF-α, (**G**) IL-6 and (**H**) CRP versus controls. Ang-(1-7) treatment prevented the increase of serum levels of TNF-α, IL-6 and CRP. (**I**) ELISA analysis of serum RF levels. The serum levels of rheumatoid factor (RF) in CIA mice were significantly elevated compared to control mice. Ang-(1-7) treatment effectively attenuated this increase versus untreated CIA mice. The results are presented as the mean ± SD (n = 5). *$p < 0.05$, **$p < 0.01$, ***$p < 0.001$.

Ang-(1-7) Inhibits Angiogenesis in the Synovial Tissue of CIA Mice

Next, we investigated the effects of Ang-(1-7) on synovial angiogenesis in an experimental arthritis model. In the CIA group, immunohistochemical staining revealed high expression of the endothelial cell marker CD31 within the synovium, whereas following Ang-(1-7) intervention, CD31 expression in the synovium was significantly reduced (Figure 3A and C). Immunofluorescence analysis revealed that the fluorescence intensity of CD31 in the synovial tissue of the CIA group was significantly increased, whereas Ang-(1-7) treatment markedly decreased the fluorescence intensity of CD31 (Figure 3B and D).

Ang-(1-7) Inhibits the Proliferation, Migration, and Tube Formation of HUVECs

To further explore the regulatory mechanism of Ang-(1-7) on angiogenesis, we stimulated HUVECs with TNF-α for in vitro experiments. Both the EdU and CCK-8 assays revealed that TNF-α promoted the proliferation of HUVECs, whereas Ang-(1-7) treatment suppressed HUVEC proliferation. The Mas receptor inhibitor A779 partially blocked the effects of Ang-(1-7) (Figure 4A–C). TNF-α also promoted the migration of HUVECs; however, following Ang-(1-7) intervention, the migration of HUVECs was significantly suppressed, and A779 partially inhibited the suppressive effect of Ang-(1-7) on cell migration (Figure 4D and E). The results from the Transwell migration assay indicated that TNF-α increased the number of HUVECs that migrated through the membrane, whereas Ang-(1-7) intervention significantly reduced the number of cells that migrated through the membrane, and A779 partially blocked the effects of Ang-(1-7) (Figure 4F and H). To assess the impact of Ang-(1-7) on the angiogenic capacity of HUVECs, we conducted a Matrigel tube formation assay and evaluated the effects of Ang-(1-7) on the tube-forming ability of HUVECs in terms of the numbers of nodes and meshes and the total branch length. Ang-(1-7) inhibited the TNF-α-induced increase in tube-forming ability, and A779 reversed the effects of Ang-(1-7) (Figure 4G, I–K). These findings suggest that Ang-(1-7) inhibits TNF-α-induced proliferation, migration, and tube formation in HUVECs via the Mas receptor.

Ang-(1-7) Inhibits the Expression of Proangiogenic Mediators

Angiogenesis is regulated by various cytokines, and we further assessed the expression of proangiogenic mediators in CIA mice and HUVECs. In vivo, immunofluorescence analysis revealed that the proangiogenic mediator VEGF was highly expressed in the synovial tissue of CIA mice and that the expression of VEGF in the synovium decreased after Ang-(1-7) intervention (Figure 5A and B). Additionally, the ELISA results revealed that Ang-(1-7) decreased the levels

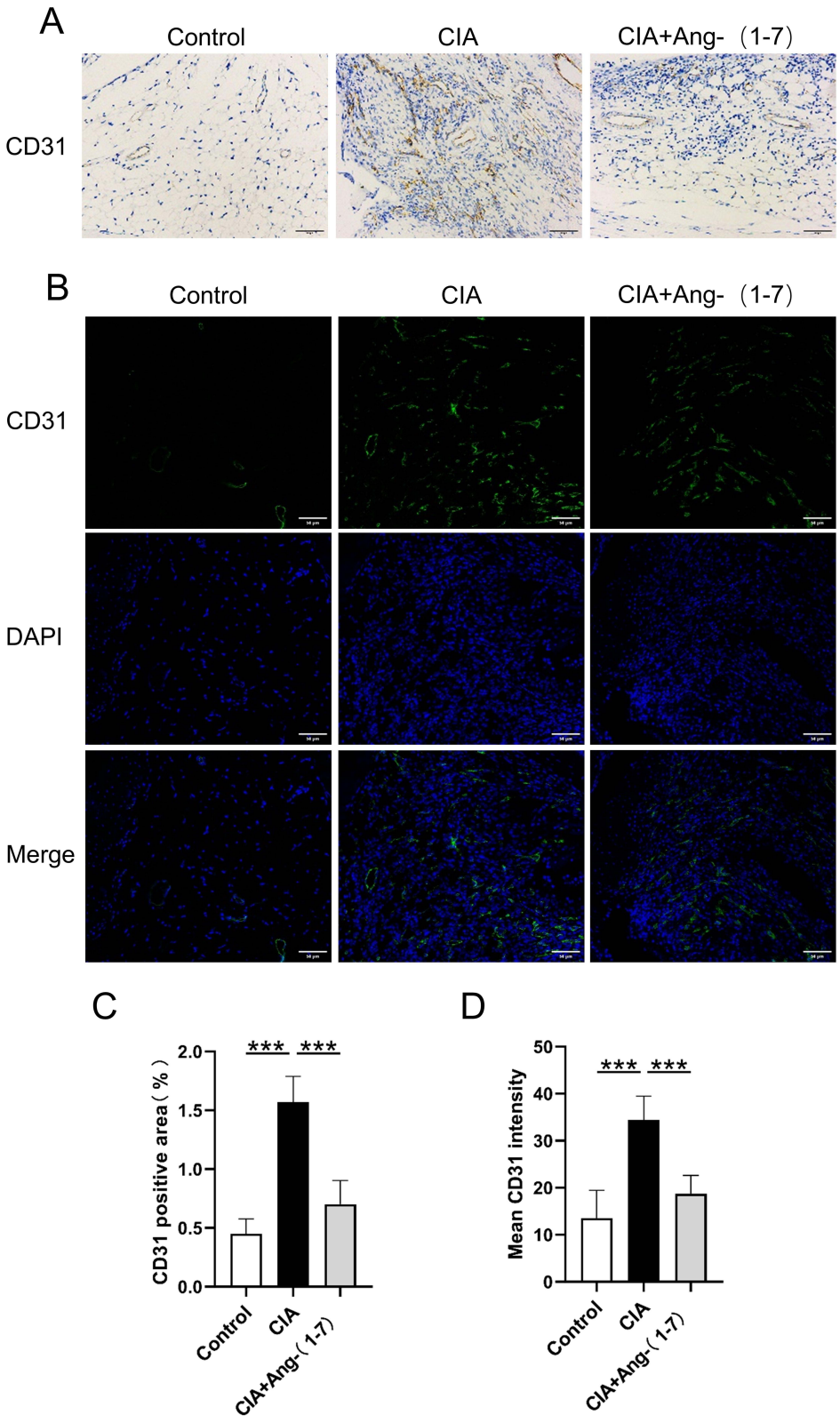

Figure 3 CD31 expression in synovial tissue of CIA mice. (**A** and **C**) Immunohistochemical staining of CD31 expression in synovial tissues of CIA mice (magnification: ×100, scale bar: 100 μm).The CD31-positive area was significantly increased in CIA mouse synovial tissue compared to controls, whereas Ang-(1-7) treatment (2 mg/kg/day) effectively reduced CD31-positive area versus untreated CIA mice. (**B** and **D**) Immunofluorescence analysis of CD31 expression in synovial tissues of CIA mice (magnification: ×200, scale bar: 50 μm). The MFI of CD31 was significantly higher in CIA mice compared to controls, whereas Ang-(1-7) treatment (2 mg/kg/day) effectively decreased CD31 MFI versus untreated CIA mice. The results are presented as the mean ± SD (n = 5). *$p < 0.05$, **$p < 0.01$, ***$p < 0.001$.

https://doi.org/10.2147/JIR.S534282

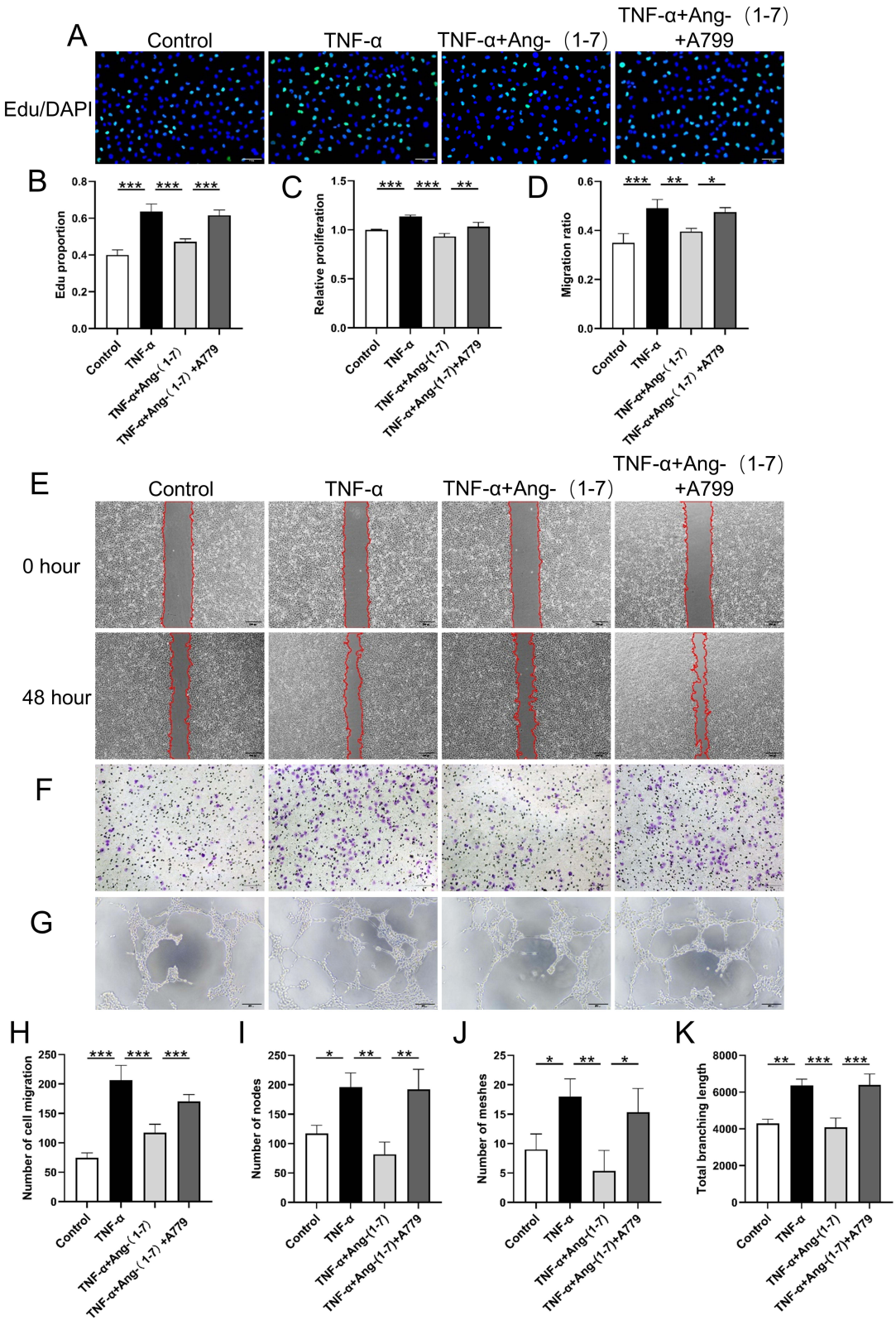

Figure 4 Ang-(1-7) inhibited TNF-α-induced proliferation, migration, and tube formation in HUVECs. HUVECs were pretreated with the Mas receptor antagonist A779 (10 μmol/L, 30 min) before cotreatment with TNF-α (10 ng/mL) and/or Ang-(1-7) (10 μmol/L) for 24 h.(**A** and **B**) Proliferation of HUVECs was measured with Edu assay. (**C**) Cell proliferation was measured using CCK8 assay. (**D** and **E**) Representative images of wound-healing assay. The histograms showed the median and the range of the migration ratio. (**F** and **H**) Representative images of transwell assay. Bar graphs displayed the median and the range of migrated cell counts per group. (**G**) Representative image of Matrigel angiogenesis assays of tube formation assay.(**I**–**K**) Quantification of nodes (**I**), meshes (**J**) and total branching length (**K**) of the tubes obtained in the in matrigel assay. Compared to the untreated HUVECs, the stimulation with TNF-α significantly enhanced HUVECs proliferation, migration, and tube formation, In contrast, Ang-(1-7) inhibited these effects. The Mas receptor antagonist A779 partially reversed Ang-(1-7)-mediated suppression.The consequences are presented as the mean ± SD of at least three independent experiments. *$p < 0.05$, **$p < 0.01$, ***$p < 0.001$.

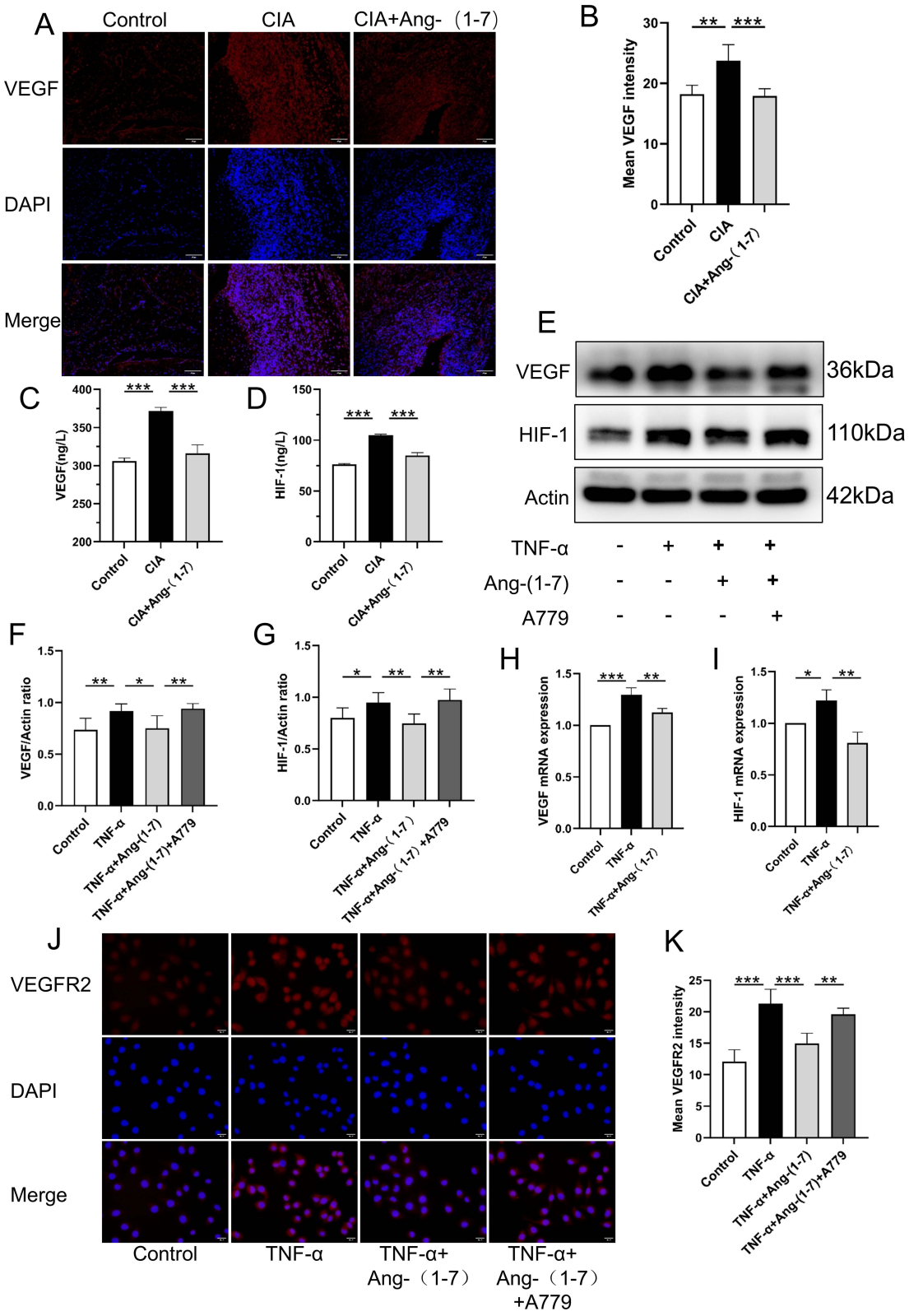

Figure 5 Effects of Ang-(1-7) on angiogenic mediators. (**A** and **B**) Immunofluorescence analysis of CD31 expression in synovial tissues of CIA mice (magnification: ×200, scale bar: 50 μm). The MFI of VEGF was significantly higher in CIA mice compared to controls, whereas Ang-(1-7) treatment (2 mg/kg/day) effectively decreased VEGF MFI versus untreated CIA mice.The results are presented as the mean ± SD (n = 5). (**C** and **D**) The serum ELISA assay of VEGF (**C**) and HIF-1 (**D**). Ang-(1-7) treatment prevented the increase of serum levels of VEGF and HIF-1 versus untreated CIA mice. (**E**–**G**) Protein levels of VEGF and HIF-1 in all groups were assessed using Western blot. Western blot analysis revealed that Ang-(1-7) significantly reduced VEGF and HIF-1 protein levels in TNF-α-stimulated HUVECs. (**H** and **I**) The mRNA level of VEGF and HIF-1 were assessed using RT-PCR. (**J** and **K**) Immunofluorescence analysis of VEGFR2 expression in HUVECs. The data are presented as the means ± standard deviation of three independent experiments. *$p < 0.05$, **$p < 0.01$, ***$p < 0.001$.

https://doi.org/10.2147/JIR.S534282

of VEGF and HIF-1 in the serum of CIA mice (Figure 5C and D). These findings indicate that Ang-(1-7) can suppress the expression of VEGF and HIF-1 in CIA mice. For in vitro experiments, we assessed the expression of VEGF and HIF-1 in HUVECs via Western blotting and qPCR. The results indicated that the protein and mRNA levels of VEGF and HIF-1 increased in TNF-α-stimulated HUVECs, whereas Ang-(1-7) treatment inhibited the protein and mRNA expression of both VEGF and HIF-1. The antagonist A779 reversed the effects of Ang-(1-7) on the protein expression of VEGF and HIF-1 (Figure 5E–I). Furthermore, we assessed the expression of the VEGF receptor VEGFR2 and found that it was highly expressed in HUVECs after TNF-α induction. Ang-(1-7) reduced the expression of VEGFR2 in HUVECs, and A779 partially reversed the effect of Ang-(1-7) (Figure 5J and K). These results suggest that Ang-(1-7) inhibits the expression of the proangiogenic factors HIF-1 and VEGF and their receptor VEGFR2 through the Mas receptor.

Ang-(1-7) Regulates the Expression of the Hippo–YAP Signaling Pathway

Previous studies have shown that the Hippo–YAP pathway influences angiogenesis by regulating endothelial cell proliferation and differentiation in various diseases. Therefore, we hypothesized that the effects of Ang-(1-7) on angiogenesis might be mediated by the Hippo–YAP pathway. We further assessed the expression of Hippo–YAP in both in vivo and in vitro experiments. The results of the immunofluorescence analysis revealed that LATS1 and YAP were highly expressed in the inflammatory synovium of CIA mice and that Ang-(1-7) inhibited the expression of LATS1 and YAP (Figure 6A–D). For in vitro experiments, Western blotting was used to assess the expression of Hippo–YAP pathway-related proteins in HUVECs. Compared with the control, intervention with TNF-α, Ang-(1-7), or A779 did not affect the total protein expression of LATS1 or YAP (Figure 6E). However, after TNF-α intervention, the expression of p-LATS and p-YAP significantly decreased, whereas Ang-(1-7) restored the protein expression of p-LATS and p-YAP. A779 inhibited the effects of Ang-(1-7) (Figure 6E–G). Immunofluorescence analysis revealed that YAP expression in the nucleus increased after TNF-α induction and that Ang-(1-7) inhibited YAP nuclear translocation, an effect that was blocked by A779 (Figure 6H). These results suggest that Ang-(1-7) may exert its effects by regulating the activation of the Hippo–YAP pathway and inhibiting YAP nuclear translocation.

Hippo–YAP Pathway Inhibitors Reverse the Antiangiogenic Effects of Ang-(1-7)

To verify that Ang-(1-7) inhibits angiogenesis through the Hippo–YAP pathway, we selected the Hippo–YAP pathway inhibitor XMU-MP-1, which exerts its inhibitory effect by suppressing the phosphorylation of mammalian STE20-like protein kinase 1 and 2 (MST1/2). Compared with TNF-α treatment, Ang-(1-7) treatment weakened the proliferative ability of HUVECs, whereas pretreatment with XMU-MP-1 promoted the proliferation of HUVECs (Figure 7A–C). Scratch assay results indicated that Ang-(1-7) reduced the migration area of HUVECs, whereas XMU-MP-1 pretreatment increased the migration ability of HUVECs (Figure 7D and E). Compared with those in the TNF-α group, the number of HUVECs that passed through the Transwell membrane in the Ang-(1-7)-treated group decreased, whereas pretreatment with XMU-MP-1 significantly increased the number of cells that passed through the Transwell membrane in the Ang-(1-7)-treated group (Figure 7F and H). Additionally, Ang-(1-7) treatment inhibited HUVEC angiogenesis, whereas XMU-MP-1 treatment enhanced the ability of HUVECs to form vessels (Figure 7G, I–K). These results indicate that the inhibitory effects of Ang-(1-7) on HUVEC proliferation, migration, and angiogenesis are mediated through the Hippo–YAP pathway.

Discussion

Rheumatoid arthritis (RA) is an immunoinflammatory disease characterized by progressive destructive joint inflammation, synovial hyperplasia, and cartilage damage. In RA, synovial tissue macrophages, synovial fibroblasts (FLSs), and mast cells become activated, releasing large amounts of inflammatory mediators such as tumor necrosis factor, interleukins, prostaglandins, chemokines, and biogenic amines. These mediators induce vasodilation and fluid extravasation, promoting the recruitment of inflammatory cells to the site of inflammation and thereby amplifying the inflammatory response.[24] This infiltrative process, along with the release of proinflammatory factors, activates endothelial cells, promoting synovial endothelial cell proliferation, migration, and invasion and forming an aggressive pannus that damages adjacent cartilage and bone tissue.[25,26] In addition to being an inflammatory disease, RA is also considered

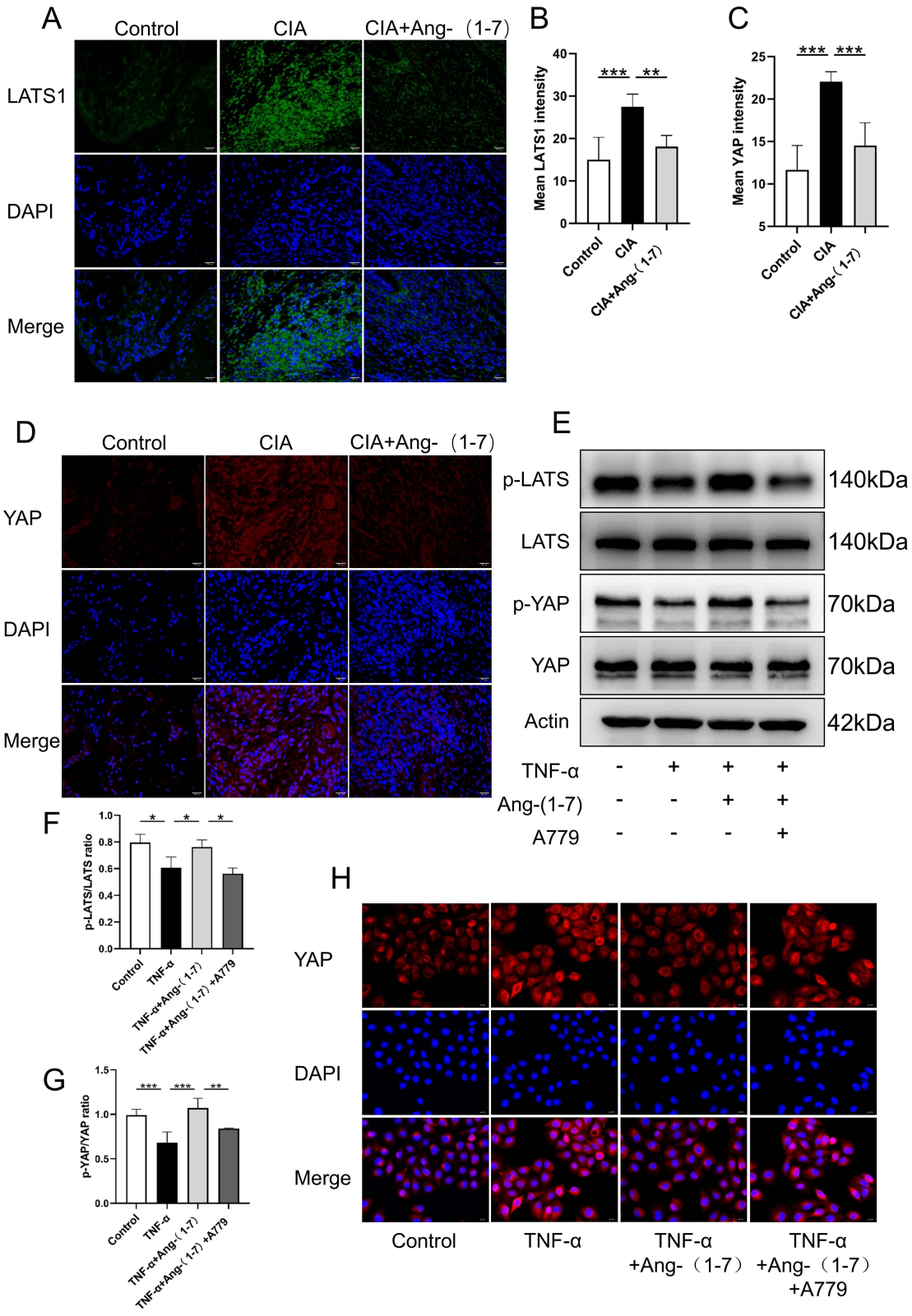

Figure 6 Ang-(1-7) modulates the expression of the Hippo–YAP signalling pathway. (**A** and **B**) Immunofluorescence analysis of LATS1 expression in synovial tissues of CIA mice (magnification: ×200, scale bar: 50 μm). (**C** and **D**) Immunofluorescence analysis of YAP expression in synovial tissues of CIA mice (magnification: ×200, scale bar: 50 μm). LATS1 and YAP MFI were elevated significantly in CIA mice versus controls, while Ang-(1-7) (2 mg/kg/day) reduced both LATS1 and YAP MFI versus untreated CIA mice. The results are presented as the mean ± SD (n = 5). ***$p < 0.001$.(**E**–**G**) Western blot analysis of LATS, p-LATS (Thr1079), YAP, and p-YAP (Ser127). (**H**) YAP nuclear translocation was assessed by upright fluorescence microscopy. Cells were immunostained with YAP antibody (labeled with TRITC, red), and nuclei were counterstained with DAPI (blue). Data are representative of three independent experiments. The results are shown as the mean ± SD (n = 3). *$p < 0.05$, **$p < 0.01$, ***$p < 0.001$.

https://doi.org/10.2147/JIR.S534282

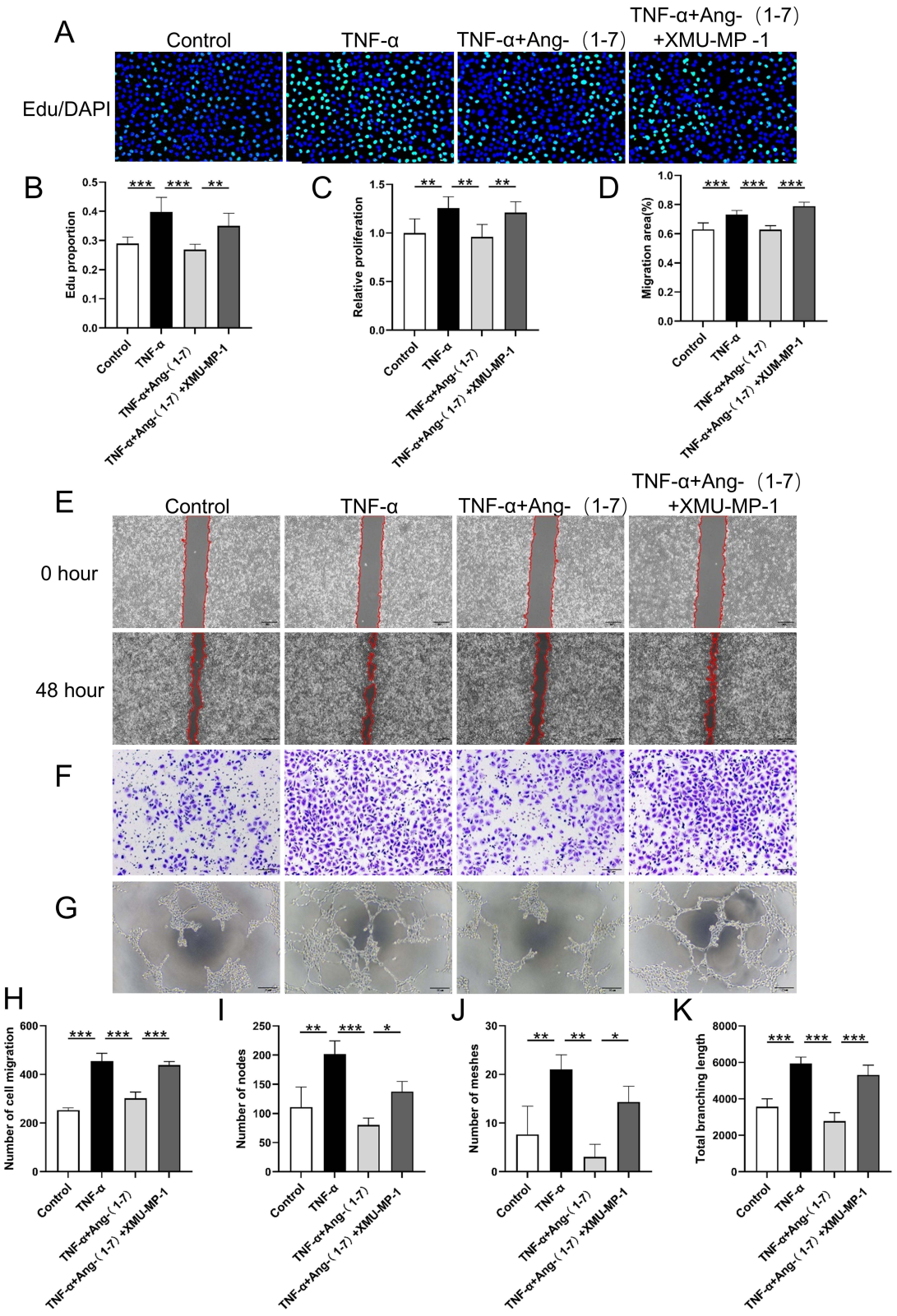

Figure 7 XMU-MP-1 antagonizes Ang-(1-7)-mediated inhibition of TNF-α-induced HUVEC activation through Hippo-YAP pathway. HUVECs were pretreated with the Hippo-YAP pathway inhibitor XMU-MP-1 (1 μmol/L, 30 min) before stimulation with TNF-α (10 ng/mL) and/or Ang-(1-7) (10 μmol/L) for 24 h. (**A** and **B**) EdU assay demonstrated that XMU-MP-1 significantly attenuated the inhibitory effects of Ang-(1-7) on TNF-α-induced HUVECs proliferation. (**C**) CCK-8 assay validated this proliferative rescue effect. (**D** and **E**) XMU-MP-1 treatment significantly increased migration area compared to Ang-(1-7) alone. (**F** and **H**) XMU-MP-1 increased migrated cell counts versus Ang-(1-7) treatment. (**G, I**–**K**) Matrigel tube formation assays (**G**) and subsequent quantification of nodes (**I**), meshes (**J**), and total branching length (**K**) revealed compromised anti-angiogenic activity of Ang-(1-7) in the presence of XMU-MP-1. The data are presented as the means ± standard deviation of three independent experiments. *$p < 0.05$, **$p < 0.01$, ***$p < 0.001$.

an "angiogenic disease" because of its close association with active tissue neovascularization.[27] Persistently generated blood vessels deliver nutrients and inflammatory cells to the RA synovium, sustaining chronic inflammation.[28] Simultaneously, neovascularization induces FLSs to adopt an invasive phenotype, promotes osteoclast activation, and leads to the release of matrix metalloproteinases, thereby creating a vicious cycle that results in joint damage, deformity, and dysfunction.[29,30] Numerous studies have demonstrated that antirheumatic drugs not only induce anti-inflammatory effects but also alleviate rheumatic disease by inhibiting angiogenesis.[31–33] Therefore, inhibiting inflammation and angiogenesis is a crucial step in RA treatment.

The ACE2/Ang-(1-7)/Mas axis is a key branch of the renin–angiotensin system that antagonizes the classic ACE/Ang II/AT1R axis.[34] Ang-(1-7) is generated by ACE2 cleavage of Ang II at the C-terminus.[35] Sana et al compared Ang II and Ang-(1-7) levels during the active and stable phases of RA. The results revealed that plasma Ang II levels were significantly elevated in patients during the active phase compared with the remission phase, and this change was accompanied by a significant decrease in Ang-(1-7) levels.[36] These findings suggest that an imbalance between the ACE/Ang II/AT1R axis and the ACE2/Ang-(1-7)/Mas axis may be involved in RA regulation. Ang II activates AT1R; increases NADPH oxidase activity; induces reactive oxygen species (ROS) production in osteoblasts, vascular smooth muscle cells, and neutrophils; and inhibits osteogenic differentiation in synovial cells. Treatment with ACE inhibitors (ACEIs) or angiotensin II receptor blockers (ARBs) has been shown to ameliorate experimental arthritis. For example, the ACEI perindopril alleviates joint damage and periarticular bone loss in CIA rats by regulating the RANKL/RANK/TRAF6 and Wnt/β-catenin signaling pathways.[37] Similarly, the AT1R antagonist losartan alleviates joint inflammation and damage by suppressing leukocyte recruitment; inhibiting the production of TNF-α, IL-1β, and chemokine ligand 1; and suppressing leukocyte–endothelial interactions.[38] Ang-(1-7), which acts as an antagonist of Ang II, induces caspase-dependent neutrophil apoptosis through the Mas receptor, promotes macrophage phagocytosis of neutrophils, inhibits neutrophil accumulation in arthritic joints, decreases inflammatory cytokine levels, and ameliorates symptoms of arthritis in model animals.[39,40] Our previous studies demonstrated that in CIA mice, Ang-(1-7) suppresses inflammation by inhibiting the NF-kB and MAPK pathways, decreasing RANKL expression, and suppressing MMP production, thereby alleviating joint destruction. This study further confirms that Ang-(1-7) not only alleviates the systemic inflammatory response and local joint inflammation in CIA mice but also effectively inhibits the production of pro-angiogenic factors, thereby blocking neovascularization in the synovial tissue. The dual inhibition of inflammation and angiogenesis fully reflects the joint protective effect.

The Mas receptor, the specific receptor for Ang-(1-7), is expressed at low levels in healthy tissues but is upregulated in pathological conditions characterized by renin–angiotensin system imbalance, including myocardial infarction and diabetes.[41,42] In these disease states, Mas1 activation counteracts the deleterious effects mediated by the ACE/Ang II/AT1R axis. Our investigations revealed Mas activation in both synovial tissues from CIA mice and TNF-α-stimulated human umbilical vein endothelial cells (HUVECs). Surprisingly, Ang-(1-7) treatment did not further increase Mas expression, despite its established role as the receptor's primary ligand. Recent studies have also shown that Mas receptor internalization occurs,[43–45] although the precise regulatory mechanisms remain undefined. While our data demonstrate that the therapeutic effects of Ang-(1-7) occur without increased Mas expression, further studies are needed to determine whether enhanced receptor internalization contributes to its mode of action.

The Hippo pathway is an evolutionarily conserved growth-inhibitory signaling pathway that plays a central role in cell proliferation and differentiation. The core of the mammalian Hippo–YAP pathway consists of a kinase cascade involving mammalian STE20-like protein kinase 1 and 2 (MST1/2) and large tumor suppressor kinase 1/2 (LATS1/2), as well as downstream effectors, the transcriptional coactivators Yes-associated protein (YAP) and transcriptional coactivator with PDZ-binding motif (TAZ).[17,18] Under physiological conditions, the Hippo pathway remains active, and YAP activity is inhibited through phosphorylation by LATS1/2. When the Hippo pathway is inactivated, dephosphorylated YAP translocates to the nucleus, where it activates the transcriptional enhancer-associated domain (TEAD) and promotes the transcription of downstream target genes, thereby driving cell proliferation.[46] Recent studies have shown that the Hippo–YAP signaling pathway plays a crucial role in the pathogenesis of RA.[47] We demonstrated dysregulated expression of the Hippo-YAP signaling pathway in synovial tissues from CIA model mice. Compared with those in normal synovial fibroblasts, the protein and mRNA expression levels of YAP and TAZ are significantly increased in RA-FLSs.[20] The proinflammatory cytokine IL-6 activates YAP via the JAK signaling pathway, promoting the formation of a YAP–Snail transcription factor complex that

drives FLS acquisition of an invasive phenotype.[48] Knockdown of YAP/TAZ induces autophagy in RA-FLSs, restricting their migration and invasion, delaying cartilage damage and bone destruction, and decreasing the severity of RA.[19] The dysregulated Hippo-YAP pathway appears to play a pivotal role in RA pathogenesis. Our findings demonstrate that Ang-(1-7) effectively restores Hippo-YAP signaling homeostasis by enhancing LATS1-mediated YAP phosphorylation, thereby inhibiting YAP nuclear translocation. Notably, the partial reversal of Ang-(1-7)'s anti-angiogenic effects by XMU-MP-1 substantiates the crucial involvement of MST1/2 activation in this regulatory mechanism. This represents the first evidence that Ang-(1-7) exerts its therapeutic effects through modulation of the Hippo-YAP pathway in RA.

The Hippo–YAP signaling pathway is also a key regulator of angiogenesis. One study indicated that, in adjuvant-induced arthritis mice, the protein Ezrin inhibited YAP phosphorylation and promoted YAP nuclear translocation, which activated the PI3K/Akt signaling pathway; promoted endothelial cell proliferation, migration, and tube formation; and increased synovial vascular formation, thereby exacerbating RA inflammation.[49] Angiogenesis is regulated by multiple cytokines, among which vascular endothelial growth factor (VEGF) and hypoxia-inducible factor 1 (HIF-1) are crucial proangiogenic mediators. In patients with RA, VEGF expression is significantly elevated in both the serum and synovial fluid. VEGF levels have been shown to correlate with RA disease activity, inflammation, and joint bone destruction.[50,51] In experimental arthritis models, preventive treatment with anti-VEGF antibodies delays arthritis onset and reduces its severity.[52] VEGF facilitates endothelial cell proliferation and migration, as well as the formation of new vascular sprouts, by activating VEGF receptor 2 (VEGFR2)-mediated intracellular signaling pathways, including PI3K/Akt and MAPK/ERK. Under hypoxic conditions, VEGF expression is upregulated via HIF-1, thereby enhancing this process. Research indicates that the increased nuclear translocation of YAP mediates the transcriptional upregulation of VEGF and HIF-1, with YAP also binding to HIF-1 to stabilize it.[53] Our study demonstrates that Ang-(1-7) may inhibit the secretion and expression of VEGF and HIF-1 by suppressing the nuclear translocation of YAP, consequently leading to a reduction in endothelial cell proliferation, migration, and tube formation.

However, our study still has some limitations. First, while the CIA model is widely used in RA research, it cannot fully replicate the complex pathophysiology of human RA. These differences limit the direct applicability of our findings to human RA. Second, the specific molecular mechanisms by which the Mas receptor regulates LATS and YAP phosphorylation require further in-depth investigation.

Conclusion

Our study is the first to demonstrate at the cellular and systemic levels that Ang-(1-7) restores Hippo–YAP pathway activity via the Mas receptor, reduces the expression of the proangiogenic mediators HIF-1 and VEGF, suppresses vascular endothelial cell activation and synovial angiogenesis, and alleviates RA inflammation, thereby protecting the joints.

Abbreviations

Ang-(1-7), angiotensin-(1-7); CIA, collagen-induced arthritis; RA, rheumatoid arthritis; HUVECs, human umbilical vein endothelial cells; VEGF, vascular endothelial growth factor; VEGFR2, vascular endothelial growth factor receptor 2; HIF-1, hypoxia-inducible factor-1; YAP, yes-associated protein; TAZ, transcriptional coactivator with PDZ-binding motif; MST1/2, mammalian STE20-like protein kinase 1 and 2; LATS1, large tumor suppressor kinase 1; FLSs, synovial fibroblasts; Ang II, angiotensin II; ACE2, angiotensin converting enzyme 2; ACEIs, angiotensin converting enzyme inhibitors; ARBs, angiotensin II receptor blockers; TEAD, transcriptional enhancer-associated domain.

Data Sharing Statement

The data are provided within the manuscript or supplementary information files.

Ethics Approval and Informed Consent

All the animal experiments were approved by the Institutional Animal Care and Use Committee of Chongqing Medical University (Approval NO. IACUC-CQMU-2023-0416) and performed in compliance with the China National Standards GB/T 35823-2018 (Laboratory Animal—Guideline for Ethical Review of Animal Welfare) and institutional regulations. No human subjects or human material were included in these studies.

Consent for Publication

Consent for publication was obtained from the participants.

Acknowledgments

This study was supported by the National Natural Science Foundation of China (81771738); the Chongqing Science and Technology Innovation Leading Talent Support Program (CQYC202104); the Program for Youth Innovation in Future Medicine, Chongqing Medical University (W0197); and the Chongqing Postdoctoral Scientific Fund Project (CSTB2023NSCQ-BHX0031).

Author Contributions

All authors made a significant contribution to the work reported, whether that is in the conception, study design, execution, acquisition of data, analysis and interpretation, or in all these areas; took part in drafting, revising or critically reviewing the article; gave final approval of the version to be published; have agreed on the journal to which the article has been submitted; and agree to be accountable for all aspects of the work.

Disclosure

The authors report no conflicts of interest in this work.

References

1. Di Matteo A, Bathon JM, Emery P. Rheumatoid arthritis. Review. *Lancet*. 2023;402(10416):2019–2033. doi:10.1016/s0140-6736(23)01525-8
2. Finckh A, Gilbert B, Hodkinson B, et al. Global epidemiology of rheumatoid arthritis. Review. *Nat Rev Rheumatol*. 2022;18(10):591–602. doi:10.1038/s41584-022-00827-y
3. Ding Q, Hu W, Wang R, et al. Signaling pathways in rheumatoid arthritis: implications for targeted therapy. Review. *Signal Transduct Target Ther*. 2023;8(1):24.68. doi:10.1038/s41392-023-01331-9
4. Maracle CX, Tas SW. Inhibitors of angiogenesis: ready for prime time? Article. *Best Pract Res Clin Rheumatol*. 2014;28(4):637–649. doi:10.1016/j.berh.2014.10.012
5. MacDonald IJ, Liu SC, Su CM, Wang YH, Tsai CH, Tang CH. Implications of angiogenesis involvement in arthritis. Review. *Int J Mol Sci*. 2018;19(7):18.2012. doi:10.3390/ijms19072012
6. Gravallese EM. Bone destruction in arthritis. Article; Proceedings Paper. *Ann Rheum Dis*. 2002;61:84–86. doi:10.1136/ard.61.suppl_2.ii84
7. Santos RAS, Sampaio WO, Alzamora AC, et al. The ace2/angiotensin-(1-7)/mas axis of the renin-angiotensin system: focus on angiotensin-(1-7). Review. *Physiol Rev*. 2018;98(1):505–553. doi:10.1152/physrev.00023.2016
8. Yu D, Huang WH, Sheng M, et al. Angiotensin-(1-7) modulates the Warburg effect to alleviate inflammation in LPS-induced macrophages and septic mice. Article. *J Inflamm Res*. 2024;17:469–485. doi:10.2147/jir.S446013
9. Sheng M, Li QK, Huang WH, et al. Ang-(1-7)/Mas axis ameliorates bleomycin-induced pulmonary fibrosis in mice via restoration of Nox4-Nrf2 redox homeostasis. Article. *Eur J Pharmacol*. 2024;962:11.176233. doi:10.1016/j.ejphar.2023.176233
10. Wang ZJ, Huang WH, Ren FF, et al. Characteristics of Ang-(1-7)/mas-mediated amelioration of joint inflammation and cardiac complications in mice with collagen-induced arthritis. article. *Front Immunol*. 2021;12:11.655614. doi:10.3389/fimmu.2021.655614
11. Lin YT, Wang HC, Chuang HC, Hsu YC, Yang MY, Chien CY. Pre-treatment with angiotensin-(1-7) inhibits tumor growth via autophagy by downregulating PI3K/Akt/mTOR signaling in human nasopharyngeal carcinoma xenografts. Article. *J Mol Med*. 2018;96(12):1407–1418. doi:10.1007/s00109-018-1704-z
12. Pei NN, Wan RQ, Chen XL, et al. Angiotensin-(1-7) decreases cell growth and angiogenesis of human nasopharyngeal carcinoma xenografts. Article. *Mol Cancer Ther*. 2016;15(1):37–47. doi:10.1158/1535-7163.Mct-14-0981
13. Ni L, Feng Y, Wan HY, et al. Angiotensin-(1-7) inhibits the migration and invasion of A549 human lung adenocarcinoma cells through inactivation of the PI3K/Akt and MAPK signaling pathways. Article. *Oncol Rep*. 2012;27(3):783–790. doi:10.3892/or.2011.1554
14. Menon J, Soto-Pantoja DR, Callahan MF, et al. Angiotensin-(1-7) inhibits growth of human lung adenocarcinoma xenografts in nude mice through a reduction in cyclooxygenase-2. Article. *Cancer Res*. 2007;67(6):2809–2815. doi:10.1158/0008-5472.Can-06-3614
15. Soto-Pantoja DR, Menon J, Gallagher PE, Tallant EA. Angiotensin-(1-7) inhibits tumor angiogenesis in human lung cancer xenografts with a reduction in vascular endothelial growth factor. Article. *Mol Cancer Ther*. 2009;8(6):1676–1683. doi:10.1158/1535-7163.Mct-09-0161
16. Liu YP, Li B, Wang XM, et al. Angiotensin-(1-7) suppresses hepatocellular carcinoma growth and angiogenesis via complex interactions of angiotensin II type 1 receptor, angiotensin II type 2 receptor and mas receptor. Article. *Mol Med*. 2015;21:626–636. doi:10.2119/molmed.2015.00022
17. Ma SH, Meng ZP, Chen R, Guan KL. The hippo pathway: biology and pathophysiology. In: Kornberg RD, editor. *Annual Review of Biochemistry, Vol 88. Annual Reviews*. 2019:577–604.
18. Boopathy GTK, Hong W. Role of hippo pathway-YAP/TAZ signaling in angiogenesis. *Front Cell Develop Biol*. 2019;7:49. doi:10.3389/fcell.2019.00049
19. Zhou W, Shen Q, Wang H, et al. Knockdown of YAP/TAZ inhibits the migration and invasion of fibroblast synovial cells in rheumatoid arthritis by regulating autophagy. Article. *J Immunol Res*. 2020;2020:11.9510594. doi:10.1155/2020/9510594
20. Caire R, Audoux E, Courbon G, et al. YAP/TAZ: key players for rheumatoid arthritis severity by driving fibroblast like synoviocytes phenotype and fibro-inflammatory response. Article. *Front Immunol*. 2021;12:16.791907. doi:10.3389/fimmu.2021.791907

21. Zhou Y, Liang P, Bi T, et al. Angiotensin II depends on hippo/YAP signaling to reprogram angiogenesis and promote liver fibrosis. *Cell. Signalling*. 2024;123:111355. doi:10.1016/j.cellsig.2024.111355
22. Chen Y, Zhu XW, Lai WF, et al. Gancao nourishing-*Yin* decoction combined with methotrexate in treatment of aging CIA mice: a study based on DIA proteomic analysis. Article. *Chin Med*. 2023;18(1):14.9. doi:10.1186/s13020-023-00709-9
23. Li T, Diao H, Zhao L, et al. Identification of suitable reference genes for real-time quantitative PCR analysis of hydrogen peroxide-treated human umbilical vein endothelial cells. *BMC Mol. Biol*. 2017;18(1):10. doi:10.1186/s12867-017-0086-z
24. Chen Z, Bozec A, Ramming A, Schett G. Anti-inflammatory and immune-regulatory cytokines in rheumatoid arthritis. Review. *Nat Rev Rheumatol*. 2019;15(1):9–17. doi:10.1038/s41584-018-0109-2
25. Alam J, Jantan I, Bukhari SNA. Rheumatoid arthritis: recent advances on its etiology, role of cytokines and pharmacotherapy. Review. *Rev Biomed Pharmacother*. 2017;92:615–633. doi:10.1016/j.biopha.2017.05.055
26. Mohr T, Haudek-Prinz V, Slany A, Grillari J, Micksche M, Gerner C. Proteome profiling in IL-1β and VEGF-activated human umbilical vein endothelial cells delineates the interlink between inflammation and angiogenesis. Article. *PLoS One*. 2017;12(6):23.e0179065. doi:10.1371/journal.pone.0179065
27. Szekanecz Z, Koch AE. Angiogenesis and its targeting in rheumatoid arthritis. Review. *Vasc Pharmacol*. 2009;51(1):1–7. doi:10.1016/j.vph.2009.02.002
28. Szekanecz Z, Besenyei T, Paragh G, Koch AE. Angiogenesis in rheumatoid arthritis. Review. *Autoimmunity*. 2009;42(7):563–573. Pii 915523014. doi:10.1080/08916930903143083
29. Maeda K, Yoshida K, Nishizawa T, et al. Inflammation and bone metabolism in rheumatoid arthritis: molecular mechanisms of joint destruction and pharmacological treatments. Article. *Int J Mol Sci*. 2022;23(5):24.2871. doi:10.3390/ijms23052871
30. Tuckermann J, Adams RH. The endothelium-bone axis in development, homeostasis and bone and joint disease. Review. *Nat Rev Rheumatol*. 2021;17(10):608–620. doi:10.1038/s41584-021-00682-3
31. Cha HS, Ahn KS, Jeon CH, Kim J, Koh EM. Inhibitory effect of cyclo-oxygenase-2 inhibitor on the production of matrix metalloproteinases in rheumatoid fibroblast-like synoviocytes. Article. *Rheumatol Int*. 2004;24(4):207–211. doi:10.1007/s00296-003-0359-3
32. Deng H, Yan CL, Xiao T, Yuan DF, Xu JH. Total glucosides of *Paeonia lactiflora* pall inhibit vascular endothelial growth factor-induced angiogenesis. Article. *J Ethnopharmacol*. 2010;127(3):781–785. doi:10.1016/j.jep.2009.09.053
33. Zhang W, Li F, Gao W. *Tripterygium wilfordii* inhibiting angiogenesis for rheumatoid arthritis treatment. Review. *J Natl Med Assoc*. 2017;109(2):142–148. doi:10.1016/j.jnma.2017.02.007
34. Ocaranza MP, Riquelme JA, García L, et al. Counter-regulatory renin-angiotensin system in cardiovascular disease. Review. *Nat Rev Cardiol*. 2020;17(2):116–129. doi:10.1038/s41569-019-0244-8
35. Rukavina Mikusic NL, Gironacci MM. Mas receptor endocytosis and signaling in health and disease. *Prog Mol Biol Transl Sci*. 2023;194:49–65. doi:10.1016/bs.pmbts.2022.09.001
36. Pour SK, Scoville C, Tavernier SS, Aghazadeh-Habashi A. Plasma angiotensin peptides as biomarkers of rheumatoid arthritis are correlated with anti-ACE2 auto-antibodies level and disease intensity. Article. *Inflammopharmacology*. 2022;30(4):1295–1302. doi:10.1007/s10787-022-01008-9
37. Wang YZ, Kou JQ, Zhang HN, et al. The renin-angiotensin system in the synovium promotes periarticular osteopenia in a rat model of collagen-induced arthritis. Article. *Int Immunopharmacol*. 2018;65:550–558. doi:10.1016/j.intimp.2018.11.001
38. Silveira KD, Coelho FM, Vieira AT, et al. Mechanisms of the anti-inflammatory actions of the angiotensin type 1 receptor antagonist losartan in experimental models of arthritis. Article. *Peptides*. 2013;46:53–63. doi:10.1016/j.peptides.2013.05.012
39. Barroso LC, Magalhaes GS, Galvao I, et al. Angiotensin-(1-7) promotes resolution of neutrophilic inflammation in a model of antigen-induced arthritis in mice. Article. *Front Immunol*. 2017;8:11.1596. doi:10.3389/fimmu.2017.01596
40. da Silveira KD, Coelho FM, Vieira AT, et al. Anti-inflammatory effects of the activation of the angiotensin-(1-7) receptor, mas, in experimental models of arthritis. Article. *J Immunol*. 2010;185(9):5569–5576. doi:10.4049/jimmunol.1000314
41. Ma YP, Yang Y, Jiang SM, et al. Angiotensin II type 1 receptor blockers favorably affect renal angiotensin II and MAS receptor expression in patients with diabetic nephropathy. Article. *J Renin-Angiotensin-Aldosterone Syst*. 2020;21(2):7.1470320320919607. doi:10.1177/1470320320919607
42. Wang J, He W, Guo LP, et al. The ACE2-Ang (1-7)-mas receptor axis attenuates cardiac remodeling and fibrosis in post-myocardial infarction. Article. *Mol Med Rep*. 2017;16(2):1973–1981. doi:10.3892/mmr.2017.6848
43. Cerniello FM, Carretero OA, Carbajosa NAL, et al. MAS1 receptor trafficking involves ERK1/2 activation through a β-arrestin2-dependent pathway. Article. *Hypertension*. 2017;70(5):982–+. doi:10.1161/hypertensionaha.117.09789
44. Cerniello FM, Silva MG, Carretero OA, Gironacci MM. Mas receptor is translocated to the nucleus upon agonist stimulation in brainstem neurons from spontaneously hypertensive rats but not normotensive rats. Article. *Cardiovasc Res*. 2020;116(12):1995–2008. doi:10.1093/cvr/cvz332
45. Wang Y, Wang J, Liu RX, et al. Severe acute pancreatitis is associated with upregulation of the ACE2-angiotensin-(1-7)-mas axis and promotes increased circulating angiotensin-(1-7). Article. *Pancreatology*. 2012;12(5):451–457. doi:10.1016/j.pan.2012.07.017
46. Fu MY, Hu Y, Lan TX, Guan KL, Luo T, Luo M. The hippo signalling pathway and its implications in human health and diseases. Review. *Signal Transduct Target Ther*. 2022;7(1):20.376. doi:10.1038/s41392-022-01191-9
47. Wang T, ZD W, WX Q, GG J, Wang G. Possible future avenues for rheumatoid arthritis therapeutics: hippo pathway. *J Inflamm Res*. 2023;16:1283–1296. doi:10.2147/jir.S403925
48. Symons RA, Colella F, Collins FL, et al. Targeting the IL-6-yap-snail signalling axis in synovial fibroblasts ameliorates inflammatory arthritis. Article. *Ann Rheum Dis*. 2022;81(2):214–224. doi:10.1136/annrheumdis-2021-220875
49. Chen QY, Fan K, Chen X, et al. Ezrin regulates synovial angiogenesis in rheumatoid arthritis through YAP and Akt signalling. Article. *J Cell Mol Med*. 2021;25(19):9378–9389. doi:10.1111/jcmm.16877
50. Sone H, Sakauchi M, Takahashi A, et al. Elevated levels of vascular endothelial growth factor in the sera of patients with rheumatoid arthritis correlation with disease activity. *Life Sci*. 2001;69(16):1861–1869. doi:10.1016/s0024-3205(01)01264-4
51. Clavel G, Bessis N, Lemeiter D, et al. Angiogenesis markers (VEGF, soluble receptor of VEGF and angiopoietin-1) in very early arthritis and their association with inflammation and joint destruction. Article. *Clin Immunol*. 2007;124(2):158–164. doi:10.1016/j.clim.2007.04.014
52. Lu J, Kasama T, Kobayashi K, et al. Vascular endothelial growth factor expression and regulation of murine collagen-induced arthritis. Article. *J Immunol*. 2000;164(11):5922–5927. doi:10.4049/jimmunol.164.11.5922
53. Zhang CX, Bian ML, Chen XR, et al. Oroxylin A prevents angiogenesis of LSECs in liver fibrosis via inhibition of YAP/HIF-1 signaling. Article. *J Cell Biochem*. 2018;119(2):2258–2268. doi:10.1002/jcb.26388